Autogenous Demineralized Dentin Matrix for Tissue Engineering Applications: Radiographic and Histomorphometric Studies

Mônica Fernandes Gomes, PhD, MD, DDS[1]/Mário James da Silva dos Anjos, PhD, MD, DDS[2]/
Terezinha de Oliveira Nogueira, PhD, MD, DDS[3]/Sérgio Augusto Catanzaro Guimarães, PhD, MD, DDS[4]

Purpose: This work evaluated the osteoconductive properties of autogenous demineralized dentin matrix (ADDM) on surgical bone defects in the parietal bone of rabbits, using the guided bone regeneration technique and polytetrafluoroethylene (PTFE) membrane. **Materials and Methods:** Surgical bone defects were created in 24 adult rabbits and repaired with either ADDM and PTFE (experimental group) or PTFE alone (control group). The ADDM had been obtained from the central incisors of the experimental rabbits. The rabbits were sacrificed after 15, 30, 60, and 90 days and the defects examined radiographically and histologically. **Results:** Radiographically, the defects in the experimental animals achieved radiopacity more quickly than the defects in the control group. **Discussion:** After 15, 30, 60, and 90 days of observation following surgery, the ADDM slices appeared to stimulate new bone formation. The dentin slices were completely incorporated into the new bone tissue and were resorbed during the bone repair. **Conclusions:** Bone repair was accelerated on the bone defects treated with ADDM when compared to the control group. (INT J ORAL MAXILLOFAC IMPLANTS 2002;17:488–497)

Key words: autogenous demineralized dentin matrix, bone repair, guided bone regeneration, polytetrafluoroethylene membrane

The repair of bone defects in the facial skeleton resulting from trauma, infection, or tumor resection is a problem for surgical and orthopedic professionals.[1–4] In the literature, several works claim the importance of decalcified dentin matrix as an osteoinductive material.[1–7] The chemotactic, mitogenic, and osteogenic potential of dentin matrix is associated with bone morphogenetic protein (BMP) according to Bessho and coworkers,[5]

[1]Professor, Department of Biosciences and Oral Diagnosis, São José dos Campos Dental School, São Paulo State University, UNESP, São José dos Campos, São Paulo, Brazil.

[2]Professor, Department of Dentistry, Ceará Federal University, Ceará, Brazil.

[3]Associate Professor, Department of Biosciences and Oral Diagnosis, São José dos Campos Dental School, São Paulo State University, UNESP, São José dos Campos, São Paulo, Brazil.

[4]Associate Professor, Research Center of the Sagrado Coração University, Bauru, São Paulo, Brazil.

Reprint requests: Dr Mônica Fernandes Gomes, Faculdade de Odontologia de São José dos Campos, UNESP, Departamento de Biociências e Diagnóstico Oral, Av. Eng. Francisco José Longo, 777, Cep: 12.245-000, São José dos Campos, São Paulo, Brazil. Fax: +55-12-39213620. E-mail: mfgomes@fosjc.unesp.br

Catanzaro-Guimarães,[7] and Gonçalves and Catanzaro-Guimarães.[8] In addition to BMP, dentin matrix is also rich in other growth factors, such as transforming growth factor-beta (TGF-beta), fibroblast growth factor (FGF), platelet-derived growth factor (PDGF), and epidermal growth factor (EGF).[1,5,8–11]

Guided bone regeneration (GBR) has been demonstrated to be successful in several clinical and experimental models.[12–16] The use of a membrane as a mechanical barrier prevents undesirable cell invasion of the bone defect during its repair, allowing preferential repopulation of this area with specific cells.[16]

The aim of this work was to evaluate the osteoconductive properties of autogenous demineralized dentin matrix (ADDM) in experimental surgical bone defects in the parietal bone of rabbits occluded with a polytetrafluoroethylene (PTFE) membrane.

MATERIALS AND METHODS

Twenty-four adult rabbits with 3.5 kg average weight were divided into 2 groups, ie, experimental (ADDM+PTFE) and control (PTFE only). The
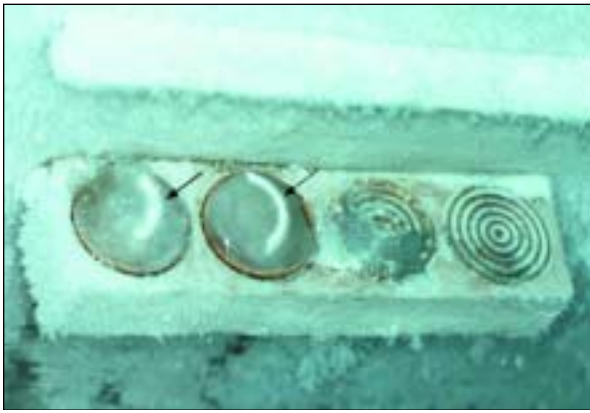
Fig 1a The ADDM *(arrows)* was placed in ice for freezing microtomy.

Fig 1b The ADDM was cut into slices of approximately 8 µm thickness with the aid of the cryostat.

ADDM was obtained by extraction of the central incisors in rabbits of the experimental group and then prepared in slices, according to Catanzaro-Guimarães and associates.[6] The pulp tissue was totally removed by the retrograde technique and the root was planed. After washing with sterile physiologic serum at 2°C, the teeth were immersed in a 0.6-N hydrochloric acid solution at 2°C until complete demineralization was achieved. The specimens were then washed during 3 hours in distilled water, under constant agitation, for total acid removal. After this process, the ADDM was cut into slices approximately 8 µm thick with the aid of a freezing microtome (Model CTD, International-Harris Cryostat/International Equipment Company, Needham Heights, MA) (Figs 1a and 1b). These slices were immersed in a special box filled with ethyl alcohol 70°/gentamicin (5 mL/0.2 sol) and stored at 2°C until the time of implantation.

An intramuscular anesthetic agent with Rompum (pre-anesthetic, Bayer AS, saúde animal, São Paulo, Brazil) and Ketalar (anesthetic, Holliday-Scott SA, São Paulo, Brazil) was administered to the animals. An incision was made in the sagittal plane of the head, followed by muscular dissection, plane to plane, and incision of the periosteum. Subsequently, a surgical bone defect was created in the parietal bone with the aid of a 5.0-mm trephine activated by a micromotor. The bone defect had an elliptical form, 1.0×0.5 cm, with a depth equal to the thickness of the removed cortical bone. In the experimental group, a PTFE membrane was positioned on the floor of the bone defect, and ADDM was placed in slices, internally and peripherally to the bone defect. The external surface of the bone defect

was completely covered by the PTFE membrane. The periosteum and muscle were then sutured as well as the skin (Figs 2a to 2d). In the control group, PTFE membrane was placed on the floor and the surface of the defect. Subsequently, the periosteum, the muscle, and the skin were sutured.

Fifteen, 30, 60, and 90 days after surgery, 3 animals of each group were sacrificed. The bone containing the surgical defect was removed en bloc, fixed in 10% formalin, and submitted to digital radiographic and light microscopic analysis for histomorphometric study. To obtain digital radiographic images of the specimens, a sensor-type image plate was utilized, and the radiographs exposed with 40-cm dff, 2 mAs, and 70 kVp. The sensor plate images were read by a laser scanner (DIGORA Digital System, Soredex, Helsinki, Finland), and these images were transferred to a computer, where they were analyzed visually and interpreted according to bone density features. The sections were obtained in the longitudinal direction and were about 8 µm thick. They were stained by hematoxylin-eosin, Mallory trichrome, and Schmorl.[17]

## Histomorphometric Analysis: Randomization of Histologic Fields

The central point of histologic section randomization and selection for histomorphometric analysis was accomplished arbitrarily, eliminating the occurrence of sampling bias. A Zeiss II reticule was placed over a compensation ocular KPL 8× Zeiss microscope (Zeiss, Thornwood, NY) to evaluate the bone density (Bd). The reticule image was superimposed on the desired histologic fields. The reticule points
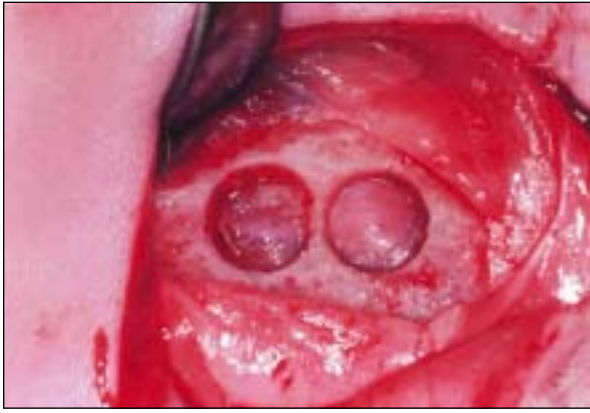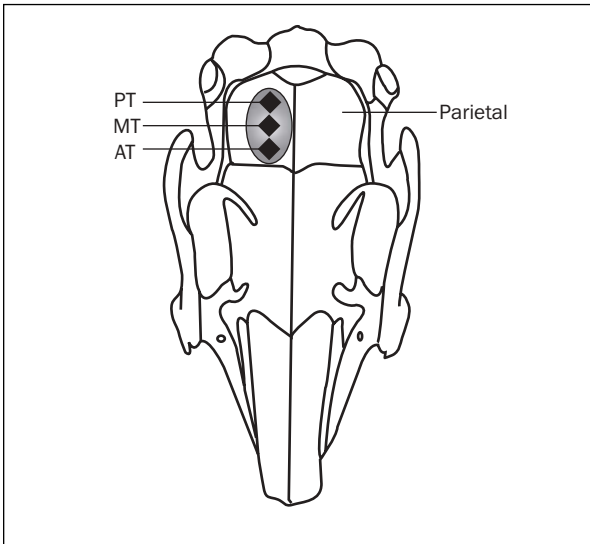
Figs 2a and 2b   A bone defect was created with the aid of a 5.0-mm trephine.

Fig 2c   In the experimental animals, a PTFE membrane was positioned on the floor of the defect and ADDM slices *(arrows)* were placed peripherally to the defect.
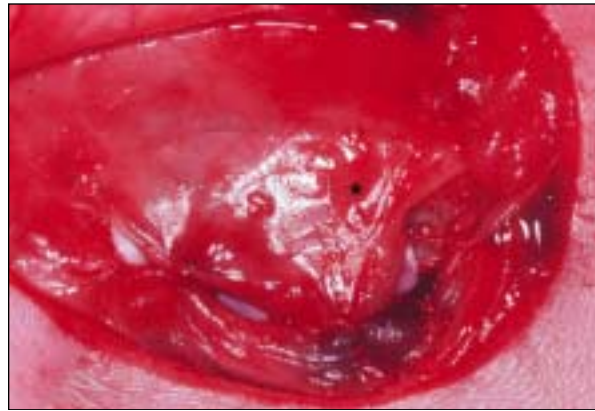
Fig 2d   The periosteum and muscle *(asterisk)* were sutured.

Fig 3   Schematic drawing of the rabbit skull with the bone defect divided into thirds. AT = anterior third; MT = middle third; PT = posterior third.

(Ni) and the total number of points over the bone defect (N) were counted. The bone density was evaluated with the following formula[18,19]: Bd = number of points in bone trabeculae (Ni)/total number of points in the bone defect (N).

During systematic randomization, histomorphometric analysis was accomplished according to the bone defect scheme (Fig 3). The chosen bone defect was submitted for examination with serial microscopy sections, from which approximately 100 sections were obtained. From these sections, 4 were randomly chosen for morphometric analysis. Subsequently, 8 histologic fields from each section in the surgical bone defect region were analyzed. At this step, a 40× objective and an ocular KPL 8× of an optical microscope (Olympus CH-2, Olympus, Tokyo, Japan) were used. The objective showed a 100-point reticule corresponding to 7,840 µm² for measuring the bone tissue area.

Figs 4a to 4d   Experimental group. Digital image of the bone defect *(arrows)* in the parietal bone of rabbit.
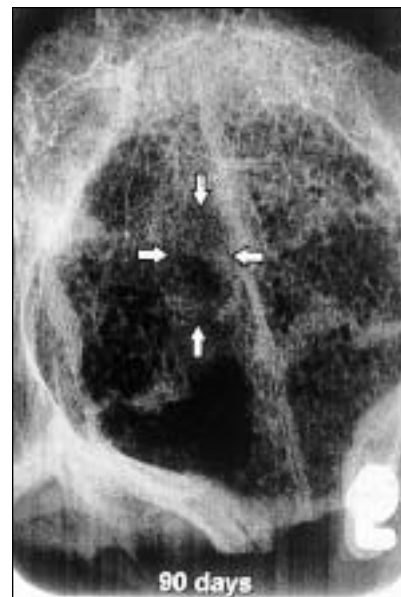
Fig 4a   *(Left)* Radiograph taken at 15 days.

Fig 4b   *(Right)* Radiograph taken at 30 days.
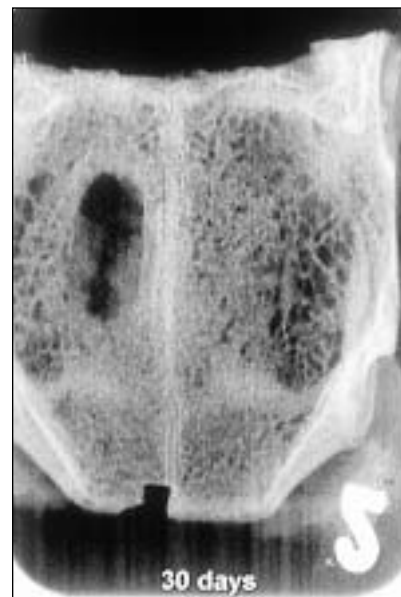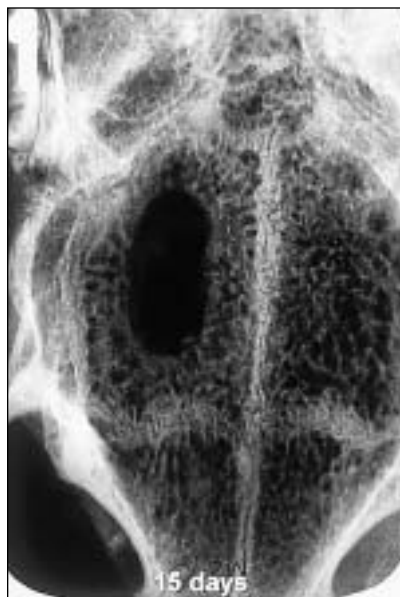
Fig 4c   *(Left)* Radiograph taken at 60 days.

Fig 4d   *(Right)* Radiograph taken at 90 days.


RESULTS

Radiographic Features

The radiographic results were analyzed as depicted in the diagram of the rabbit skull (Fig 3):

Experimental Group. During the 15-day observation period, a well-delineated and radiolucent area suggestive of a bone defect was observed (Fig 4a). At 30 days, a homogeneous radiopaque area around the bone defect, with density similar to normal bone tissue, was seen in the anterior and middle thirds (Fig 4b). The middle third showed greater radiopacity than the anterior third and the latter greater radiopacity than the posterior third. At 60 days, a radiopaque tissue of variable density filled the bone defect (Fig 4c). The areas around the surgical defect showed visually greater density than the central portion of the defect, as well as similar density to the normal bone tissue. At 90 days, the bone defect region had been replaced by a radiopaque area with a density similar to the normal bone tissue around and on a digital image of the bone defect area, where a normal trabecular bone arrangement was observed (Fig 4d).

Control Group. During the 15-day observation period, a radiolucent, homogeneous area involving

Figs 5a to 5d Control group. Digital image of the bone defects *(arrows)* in parietal bone of rabbit.
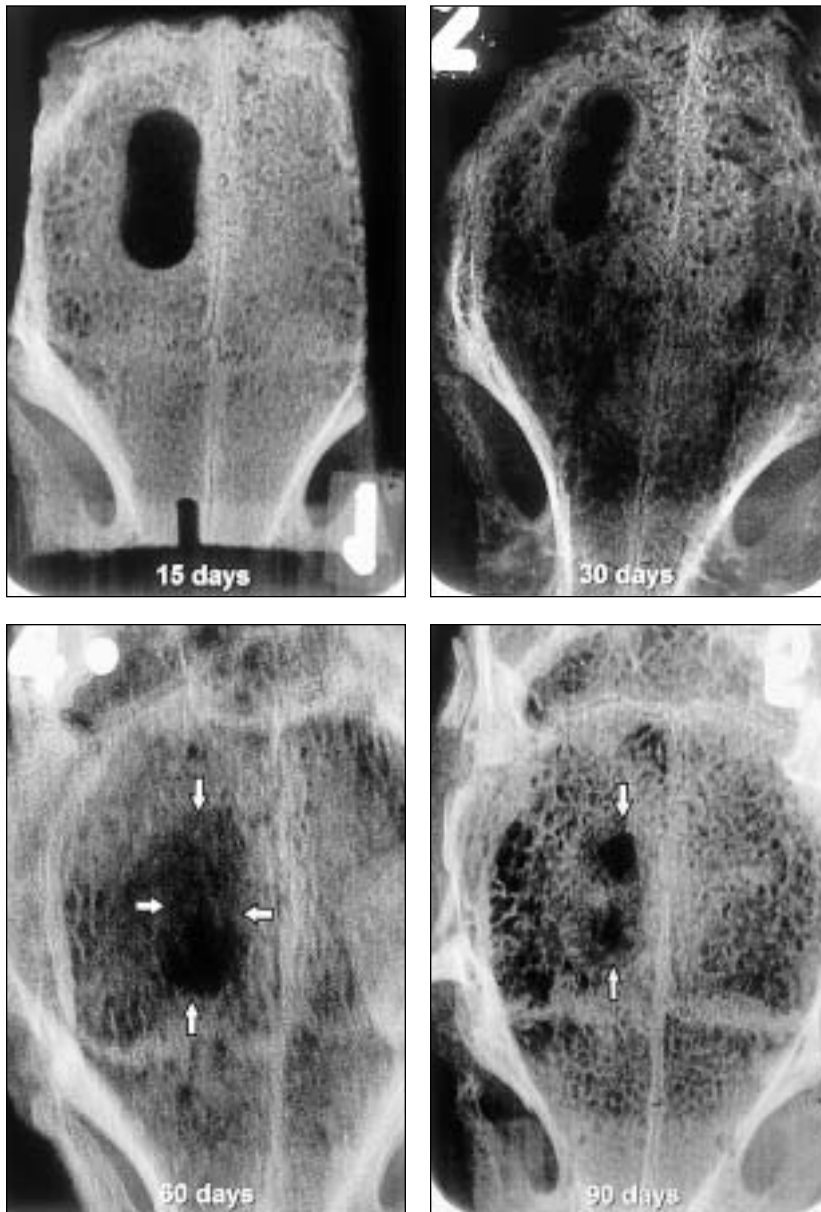
Fig 5a *(Left)* Radiograph taken at 15 days.

Fig 5b *(Right)* Radiograph taken at 30 days.

Fig 5c *(Left)* Radiograph taken at 60 days.

Fig 5d *(Right)* Radiograph taken at 90 days.

all of the bone defect, with less density than the normal bone tissue, was apparent. The 3 sections of the defect showed similar radiolucency. At 30 days, a small radiopaque area with variable density was observed around the bone defect in the middle and posterior thirds. The anterior third showed lower density than the middle and posterior thirds, and the middle third presented greater density than the posterior third and less density than the normal bone tissue around the defect. The limits of the defect were still irregular. At 60 days, the bone defect area was radiopaque, with density similar to normal bone tissue. On the anterior third, a dis-

crete, irregular, and non-delineated radiolucent image was also observed, with lower density than the normal bone. The bone defect was no longer delineated. At 90 days, the bone defect area was radiopaque, with density similar to the normal bone tissue. In addition, 2 radiolucent areas were present, with different size and density, on the anterior and posterior thirds (Fig 5).

Microscopic Features

Experimental Group. At 15 days, the bone defect was filled by bone tissue with immature trabeculae and osteogenic connective tissue (Fig 6). In certain

Fig 6 Experimental sample at 15 days. The bone defect *(arrows)* is filled by bone tissue with immature trabeculae and connective tissue (hematoxylin-eosin; magnification ×25).
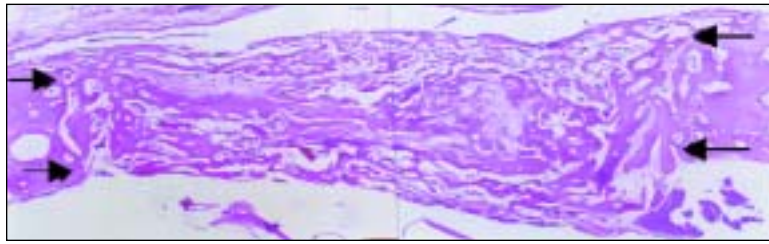
Fig 7 Experimental sample at 15 days. Deposition of newly formed bone matrix on the surface of the ADDM slices *(asterisk)* is evident (Mallory trichromic; magnification ×200).
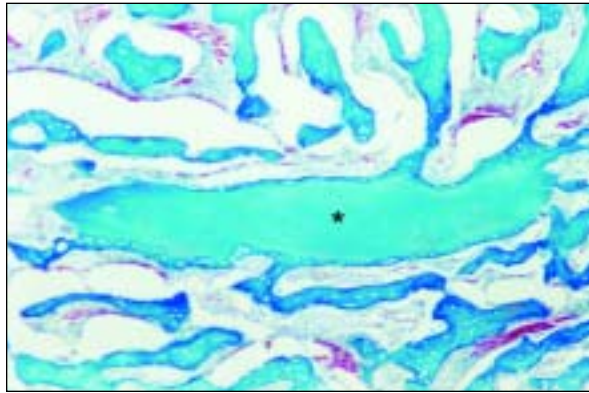
Fig 8 Experimental sample at 30 days. The bone defect *(arrows)* is filled by new bone formation characterized by homogeneous and exophytic bone growth (hematoxylin-eosin; magnification ×25).
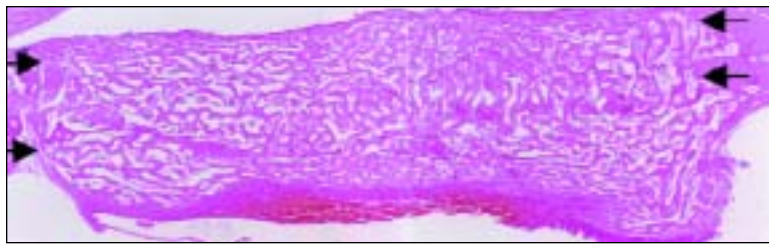
areas, intimate contact of the osteoblastic cells with the ADDM slices, the deposition of bone matrix on the surface of the ADDM slices surface, and their incorporation with the newly formed bone trabeculae, were observed (Fig 7). In addition, no rejection reaction to the ADDM slices was noted.

At 30 days, in a panoramic view, it was evident that the bone defect was filled by bone tissue characterized by homogeneous and exophytic bone growth (Fig 8). In the central region and at the extremities of the defect, scarce osteogenic connective tissue with no inflammatory cell infiltrate was observed. The bone tissue appeared to be either immature or mature, either thick or thin and irregular. The presence of red bone marrow within medullary spaces was found. The ADDM slices located on the extremities of the defect were incorporated into the newly formed bone matrix. The presence of odontoblastic processes inside the dentinal tubule of the ADDM slices was noted. Osteoblasts and osteoclasts populated the ADDM slice surface. Osteoblasts were associated with bone

matrix in intimate contact with the ADDM slices (Figs 9a and 9b). No inflammatory cell infiltrate was found next to the ADDM slices.
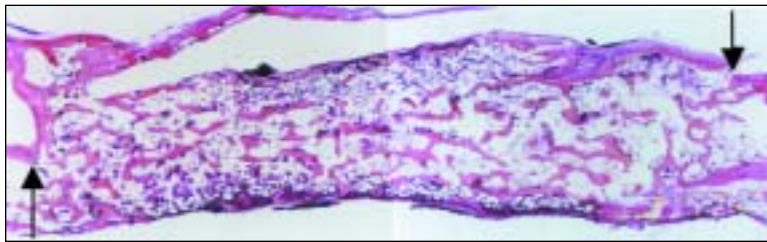
At 60 days, the bone defect was totally filled by bone tissue, showing mature and well-delineated bone trabeculae. However, their distribution was irregular, with large medullary spaces. The cortical bone was poorly defined. During this period, no presence of ADDM slices was seen. The medullary spaces were large, with yellow bone marrow. In a panoramic view, it was observed that the newly formed bone tissue exceeded the limits of the pre-existent cortical bone (Fig 10).

At 90 days, the bone defect had been replaced by bone tissue, with many mature bone trabeculae and large medullary spaces. In some areas, trabeculae with many cells included were either thick or thin and irregular. In a panoramic view, the defect area was thicker than the surrounding regular bone (Fig 11).
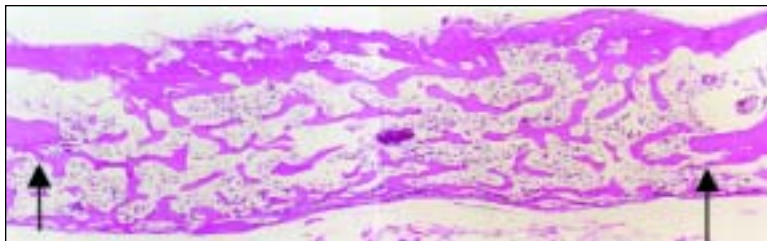
Control Group. At 15 days, the surgical bone defect was filled by connective tissue and some bone trabeculae. The immature bone tissue appeared thin
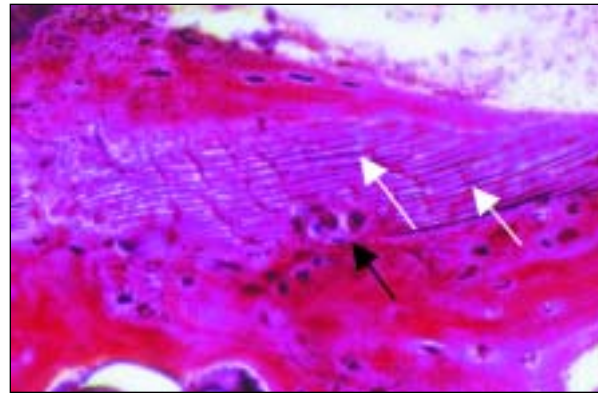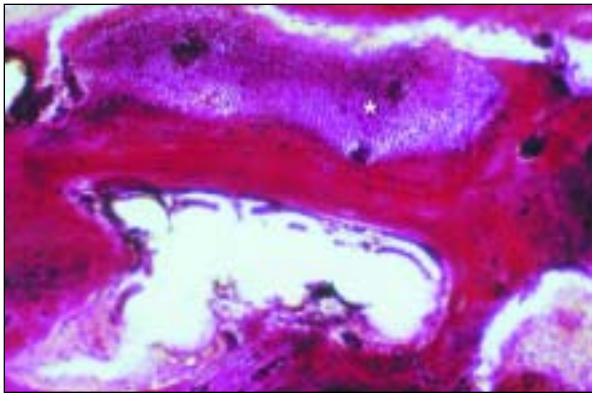
Figs 9a and 9b   Experimental sample at 30 days. *(Left)* Bone matrix is in contact with ADDM *(asterisk)* and *(right)* odontoblastic processes inside the dentinal tubules *(white arrows)* of the ADDM slices and osteocytes and osteoclasts *(black arrows)* on the surface of the ADDM slice (Schmorl; magnification ×200 and ×400, respectively).

Fig 10   Experimental sample at 60 days. The bone defect region *(arrows)* was totally filled by bone tissue, showing mature and well-delineated bone trabeculae and large medullary spaces (Schmorl; magnification ×25).

Fig 11   Experimental sample at 90 days. The bone defect region *(arrows)* was replaced by bone tissue, with many mature bone trabeculae and large medullary spaces (hematoxylin-eosin; magnification ×25).
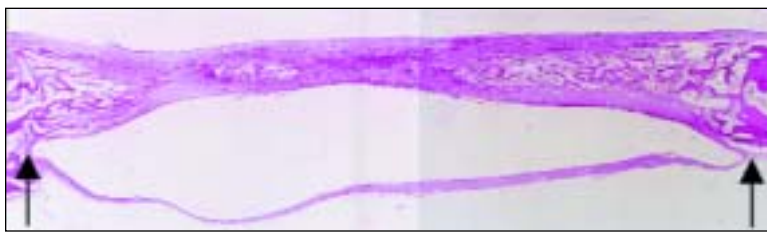
Fig 12   Control sample at 15 days. The surgical bone defect *(arrows)* was filled with connective tissue and some immature bone trabeculae located at the limits of the defect, toward the central region (hematoxylin-eosin; magnification ×25).

and irregular and was located at the limits of the defect, toward the central region of surgical bone defect. The few bone trabeculae of the central region were thinner compared with the trabeculae at the periphery of the bone defect, characterizing centripetal bone growth (Fig 12).
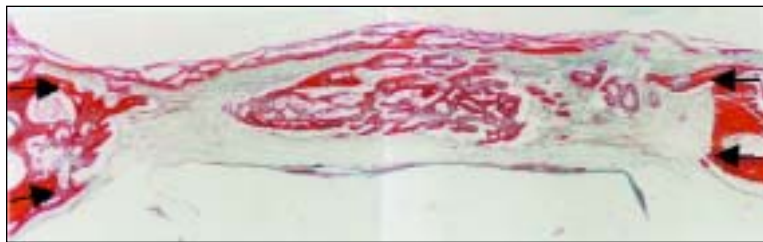
At 30 days, bone tissue and connective tissue filled the defect. Microscopically, the presence of a bone tissue mass was observed at the central portion and connective tissue at the periphery of the bone defect. There was no inflammatory cell infiltrate in this connective tissue. In a panoramic view, immature bone trabeculae intermingled with connective

tissue in the extremities of the defect were seen. The newly formed bone tissue showed centripetal growth (Fig 13).

At 60 days, bone tissue and connective tissue filled the bone defect area. The bone tissue was less mature in the central portion and more mature at the periphery of the defect. In a panoramic view, medullary spaces were evident (Fig 14).

At 90 days, the bone defect was totally filled by mature bone tissue and large medullary spaces. In a panoramic view, newly formed and well-defined cortical bone was seen, similar to the cortical bone level of the surrounding regular bone (Fig 15).

Fig 13 Control sample at 30 days. The defect region *(arrows)* was filled with bone tissue and connective tissue (Mallory trichromic; magnification ×25).

Fig 14 Control sample at 60 days. The defect region *(arrows)* was filled with bone tissue, connective tissue, and medullary spaces (hematoxylin-eosin; magnification ×25).
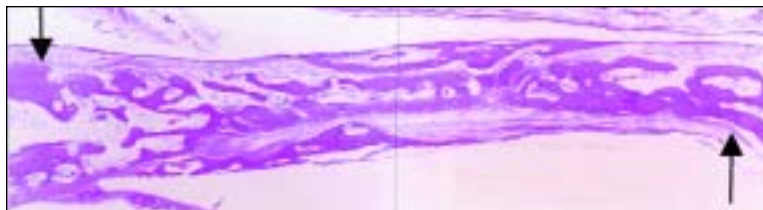
Fig 15 Control sample at 90 days. The bone defect region *(arrows)* was completely filled with bone tissue, with few mature bone trabeculae and large medullary spaces (Mallory trichromic; magnification ×25).
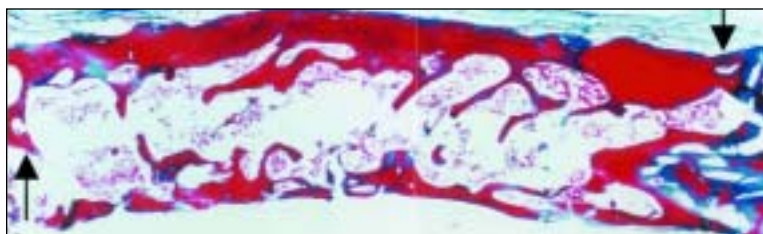
Fig 16 Representation of the volume of bone trabeculae of bone tissue formed during the process of bone repair in the different observation times of the experimental and control groups. Bone density = number of bone trabeculae (Ni)/8×100-point reticule area (N).
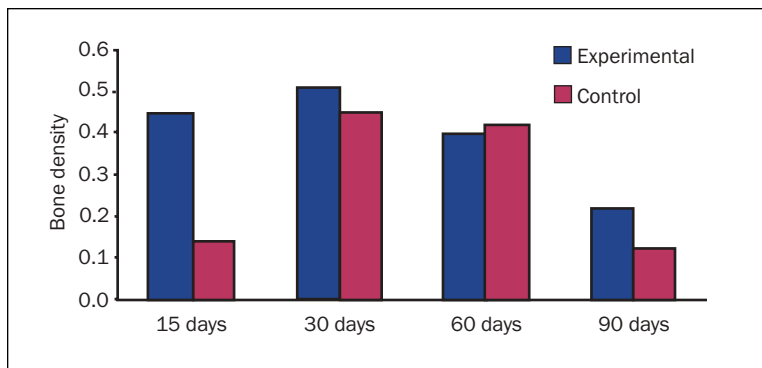
Histomorphometric Analysis

The purpose of this analysis was to measure bone density in the area of new bone tissue in the process of evolution of bone repair after implantation of decalcified dentin matrix into the bone defect, according to the formula for determining the bone density presented in the Methods section. The analysis of the results, shown in Fig 16, demonstrated that the bone defect implanted with ADDM presented a larger quantity of bone tissue compared to the control group at the time points of 15, 30, and 90 days.

DISCUSSION

Many investigators have studied different types of osteoinductive and/or osteoconductive materials trying to find materials or substances that could accelerate the bone repair process. Among the various materials found in the literature, ADDM in bone defects has shown excellent results, since it has osteogenic properties and can be resorbed during the bone remodeling process in the host area.[1–4,6,7]

Osteoinduction has been described as a differentiation phenomena of mesenchymal cells into

osteoprogenitor or osteoprecursor cells and, therefore, the newly formed bone tissue can develop through intramembranous ossification.[20] Some research has shown the formation of cartilaginous and bone tissue after implantation of demineralized dentin in the intramuscular region of laboratory animals. This phenomenon occurs as the result of the presence of an osteoinductor substratum of the dentin matrix.[21–24] The preparation process for ADDM followed in this work was recommended by Gonçalves,[1] Gomes and coworkers,[2] Carvalho,[3] Gomes and associates,[4] Catanzaro-Guimarães and colleagues,[6] Gonçalves and Catanzaro-Guimarães,[8] and Butler and coworkers.[22] It probably did not impair the activity of the BMP present in the dentin matrix, as a higher volume of bone tissue was verified in the experimental groups than in the control groups.

The radiographic and histomorphometric results showed that, during the 15-day period, the surgical defect of the experimental group demonstrated greater radiopacity, lesser radiolucency, and a larger quantity of bone tissue with the presence of more osteoblasts than the control group. This could be related to the osteoinductive property of the ADDM slices, which appeared to be well incorporated in the newly formed bone matrix. These findings were previously reported by Gonçalves,[1] Carvalho,[3] Gomes and coworkers,[4] and Catanzaro-Guimarães and associates.[6] At the 30-day period, the experimental group exhibited more homogeneous centripetal bone growth with more radiopaque limits than the control group. This occurred apparently because of the presence of the ADDM, which probably provided a stimulus to the osteogenic cells at the limits of the bone defect. This might represent ADDM osteoinductive activity, as observed by Gonçalves,[1] Gomes and associates,[2,4] Carvalho,[3] and Catanzaro-Guimarães and coworkers.[6] ADDM slices appeared to have stimulated new bone formation, producing a greater amount of bone tissue in the experimental group than in the control group. In a panoramic view, it was observed that the tissue thickness of the bone defect area of the control group was less than that of the experimental group. In both groups, no signs of inflammatory cell infiltrate were seen. During the 60-day period, in the experimental group, the bone trabeculae were visually homogeneous and the medullary spaces were larger when compared with the control group. The bone defect was filled by bone tissue, which was as evident as in the control group. During the bone remodeling process, the ADDM slices had been resorbed. At the 90-day period, the radiopacity of the defect treated with ADDM was greater than in the control group.

Microscopically, it was observed that the bone defect was totally filled by bone tissue in both groups.

Throughout the observation period, the PTFE membranes remained intact.

There was no rejection of ADDM in the present study, as shown by Gonçalves,[1] Gomes and coworkers,[4] Catanzaro-Guimarães and associates,[6] and Catanzaro-Guimarães.[7] According to Catanzaro-Guimarães and colleagues,[6] Catanzaro-Guimarães,[7] and Bang,[21] this could be the result of the low antigenicity of ADDM.

ADDM may have presented chemotactic properties, attracting osteoprogenitor cells and osteoblasts to the region where ADDM slices were present, thus promoting acceleration of the bone repair. According to Gomes and associates,[4] Catanzaro-Guimarães and coworkers,[6] Gonçalves and Catanzaro-Guimarães,[8] Robert-Clark and Smith,[11] and Urist and Strate,[25] such a phenomenon likely occurs because of the release of BMP and other growth factors from the dentin matrix, showing their possible properties as osteoinductive and osteoconductive material.

CONCLUSIONS

The ADDM slices showed osteoconductive properties. ADDM was completely incorporated in the newly formed bone tissue and resorbed during the bone remodeling process. Bone repair was accelerated in the experimental group when compared to the control group.

ACKNOWLEDGMENT

REFERENCES

1. Gonçalves EAL. Study of the Process of Bone Repair in Surgical Defects Implanted with Demineralized Autogenous Dentin Matrix in Radius of Dogs [thesis]. Bauru: University of São Paulo, 1997.
2. Gomes MF, Silva MJS, Nogueira TO, Tavano O, Catanzaro-Guimarães SA. Implantation of dentin matrix in skull defects using amniotic membrane [abstract]. J Dent Res 1999;78:363.
3. Carvalho VAP. Effects of the Demineralized Homogeneous Dentin Matrix in Bone Repair in Mandibles of Rabbits: Histomorphometric Analysis [thesis]. Piracicaba: University of Campinas, 2001.

4. Gomes MF, Silva MJS, Nogueira TO, Catanzaro-Guimarães SA. Histologic evaluation of the osteoinductive property of autogenous demineralized dentin matrix on surgical bone defects in rabbit skulls using human amniotic membrane for guided bone regeneration. Int J Oral Maxillofac Implants 2001;16:563–571.

5. Bessho K, Tagawa T, Murata M. Purification of rabbit bone morphogenetic protein derived from bone, dentin, and wound tissue after tooth extraction. J Oral Maxillofac Surg 1990;48:162–169.

6. Catanzaro-Guimarães SA, Catanzaro-Guimarães B, Garcia RB, Alle N. Osteogenic potential of autogenic demineralized dentin implanted in bony defects in dog. Int J Oral Maxillofac Surg 1986;15:160–169.

7. Catanzaro-Guimarães SA. Possibility to reinforce bone repair with decalcified dentin matrix. In: Gesellschaft für Orale Implantologie (eds). Jahrbuch für Orale Implantologie. Berlin: Quintessenz, 1993:33–34.

8. Gonçalves EL, Catanzaro-Guimarães SA. Proteínas morfogenéticas ósseas: Terapêutica molecular no processo de reparo ósseo. Rev Odont Universidade de São Paulo 1998; 12:299–304.

9. Bessho K, Tagawa T, Murata M. Comparison of bone matrix-derived bone morphogenetic proteins from various animals. J Oral Maxillofac Surg 1992;50:496–501.

10. Tziafas D. Induction of odontoblast-like cell differentiation in dog dental pulps after in vivo implantation of dentine matrix components. Arch Oral Biol 1995;40:883–893.

11. Robert-Clark DJ, Smith AJ. Angiogenic growth factors in human dentin matrix. Arch Oral Biol 2000;45:1013–1016.

12. Bluhm AE, Laskin DM. The effects of polytetrafluoroethylene cylinders on osteogenesis in rat fibular defects: A preliminary study. J Oral Maxillofac Surg 1995;53:163–166.

13. Karring T, Nyman S, Gottlow J, Laurell L. Development of the biological concept of guided tissue regeneration-animal and human studies. Periodontol 2000 1993;1:26–35.

14. Buser D, Dahlin C, Schenk RK. Guided Bone Regeneration in Implant Dentistry. Berlin: Quintessence, 1994.

15. Nyman S, Lang NP. Guided tissue regeneration and dental implants. Periodontol 2000 1994;4:109–118.

16. Nyman R, Magnusson M, Sennerby L, Nyman S, Lundgren D. Membrane-guided bone regeneration: Segmental radius defects studied in the rabbit. Acta Orthop Scand 1995;66: 169–173.

17. Raphael SS. Lynch's medical laboratory technology. Philadelphia: Saunders, 1976:940.

18. Taga R, Stipp ACM. Practical Handbook of Morphometry to Light Microscopy. Planning and Development of an Experiment [thesis]. Bauru: University of São Paulo, 1994.

19. Partiff AM. Bone histomorphometry: Proposed system for standardization of nomenclature, symbol, and unit. Calcif Tissue Int 1988;42:284–286.

20. Friedenstein AJ. Precursor cells of mechanocytes. Int Rev Cytol 1976;47:327–359.

21. Bang G. Induction of heterotopic bone formation by demineralized dentin in guinea pig: Antigenicity of the dentin matrix. J Oral Pathol Med 1972;1:172–185.

22. Butler WT, Mikulski A, Urist MR. Noncollagenous proteins of rat dentin matrix possessing bone morphogenic activity. J Dent Res 1977;56:228–232.

23. Gould TR, Westbury I, Tillman J. Dentin matrix gelatin (DMG) as a possible universal grafting material in periodontics. J Periodontol 1982;53:22–25.

24. Kawai T, Urist MR. Bovine tooth-derived bone morphogenetic protein. J Dent Res 1989;68:1069–1074.

25. Urist M, Strate BS. Bone morphogenetic protein. J Dent Res 1971;50:1392–1406.